

## Investigation of Corrosion Inhibition Properties of Caffeine on Nickel by Electrochemical Techniques

M. Ebadi<sup>1,2,\*</sup>, W. J. Basirun<sup>1</sup>, S. Y. Leng<sup>1,3</sup> and M. R. Mahmoudian<sup>1,4</sup>

<sup>1</sup> Department of Chemistry, Faculty of Science, University of Malaya, 50603 Kuala Lumpur, Malaysia.

<sup>2</sup> Department of Chemistry, Faculty of Sciences, Islamic Azad University- Gorgan Branch, Gorgan, (IRAN).

<sup>3</sup> Department of Chemical Science, Faculty of Science, University Tunku Abdul Rahman, Jalan Universiti, Bandar Barat, 31900 Kampar, Perak, Malaysia.

<sup>4</sup> Department of Chemistry, Masjed-Soleiman Branch, Islamic Azad University, Masjed- Soleiman, Iran.

\*E-mail: [mehdi\\_2222002@yahoo.com](mailto:mehdi_2222002@yahoo.com)

Received: 15 June 2012 / Accepted: 29 July 2012 / Published: 1 September 2012

---

The corrosion behaviour of Ni surface in the absence and presence of caffeine in 3.5% NaCl solution is studied using electrochemical impedance spectroscopy, open circuit potential, electrochemical noise analysis and linear scan voltammetry. The corrosion rate of the nickel surface decreases and the inhibition efficiency increases from 93.7% to 96.8% with the increase of caffeine in the corrosive solution. The FESEM images show that the caffeine addition in the corrosive solution reduces the formation of pits and cavities on the nickel surface.

---

**Keywords:** Caffeine, electro-corrosion techniques, inhibitor efficiency, nickel

### 1. INTRODUCTION

Nickel is an important metal with wide industrial applications due to its excellent properties. The main applications of nickel are in electronic devices, for the production of nano-wires, nano-sheets, nano-tubes and as finishing layers in the automotive industry. Nickel has good corrosion resistance in atmospheric and in other aggressive media such as acids and alkalis [1, 2]. For this reason, nickel and nickel alloys electrodeposition are important process to provide a surface finish for better corrosion protection [2-6]. To improve the corrosion resistance of nickel, several types of organic and inorganic compounds were investigated as inhibitors against corrosion [5-8]. The organic compounds studied as inhibitors are azoles [9-14], amines [15-17], and amino acids [18-20]. These

typical inhibitors incorporate atoms such as nitrogen, sulphur and phosphorous. Caffeine [1, 2, 5] (trimethylxanthine) was investigated by Fallavena et al. [21] and found that the copper surface can be protected from corrosion in a potassium nitrate solution with the addition of caffeine. Rajendran et al. [22] studied the corrosion inhibition properties of  $Zn^{2+}$ -caffeine complex on mild steel immersed in an aqueous corrosive solution and showed that the inhibition efficiency ( $IE$ ) increased with the addition of the  $Zn^{2+}$ -caffeine complex. Nickel electrodeposition in the presence of a magnetic field also increased its corrosion resistance compared to deposition without a magnetic field [1, 2]. Nickel-cobalt alloy electrodeposition also improves the corrosion resistance compared to the single metal [1-4].

Electrochemical techniques are powerful tools to study the influence of inhibitors on the corrosion resistance of metal surface. Electrochemical DC techniques such as electrochemical noise analysis (ENA), open circuit potential (OCP), and Tafel are tools which can provide information about the efficiency of the inhibitors in the corrosive environment. The performance of the inhibitors against corrosion can be determined from the corrosion rate measurements in different conditions [14-22]. Electrochemical impedance spectroscopy (EIS) is another powerful tool to investigate the surface of the corroding metal and supplements the DC methods [22-28]. In this work, the corrosion behaviour of Ni in 3.5% NaCl solution with different concentrations of caffeine is studied using a combination of AC method (EIS) and DC methods (OCP, Tafel, and ENA). All these tools are established techniques to study the performance of the organic inhibitors in corrosive solutions [29].

## 2. EXPERIMENTAL

All experiments were done using Nickel plates (99.9% purity) in an aqueous 3.5% NaCl solution containing different concentrations of caffeine. The Ni plates ( $0.2 \times 1 \times 1$  cm) were polished with emery paper (2000 grit), rinsed in distilled water and ultrasound in acetone to remove oily stains. A three-compartment cell with a saturated calomel electrode (SCE) as the reference electrode and Ni plates with equal surface area was used as the working and counter electrodes for the corrosion measurements. Frequency response analysis (FRA) software was used in the EIS experimental and simulation experiments while general purpose electrochemical software (GPES) was used in the linear scan voltammetry (LSV) to find Tafel plots, open circuit potential (OCP) and electrochemical noise analysis (ENA) techniques. A computer interfaced with an Autolab (302N) Potentiostat/Galvanostat instrument was used to perform the experiments and simulations. The scan rate for LSV was  $10 \text{ mV s}^{-1}$  between 0.3 V to -0.5 V while the EIS measurements were carried out at the OCP value with a frequency range of 100 kHz-10 mHz with an amplitude of 5 mV around the OCP value. The ENA was operated at the OCP value for 1675 s. Prior to all analysis (EIS, ENA, and LSV) the Ni plates were immersed in the corrosive solution (3.5% NaCl) containing different amounts of caffeine for 1 h to obtain the OCP value. Field emission scanning electron microscopy (FESEM) with a JEOL JSM-840A instrument was used to capture the images of the nickel surface after immersion in the corrosive solution.

### 3. RESULTS AND DISCUSSION

#### 3.1. OCP/ EIS studies

A model of nickel dissolution in sulphuric acid medium was proposed by Sato and Okamoto [30, 31] as:



The subscripts “ad” and “sol” refers to the species which adsorb on the electrode surface and dissolve in the solution phase respectively. Keddam et al. [32] suggests that the dissolution of nickel depends on the anion which binds to the nickel in both phases. Following the model proposed by Sato and Okamoto, a two-step model of the nickel dissolution process with the presence of the  $\text{Cl}^-$  ions can be written as:



To study the influence of caffeine on the corrosion behaviour of the nickel surface in chloride medium, open circuit potential (OCP) measurements were done on four solutions with different concentrations of caffeine in 3.5% NaCl solution.

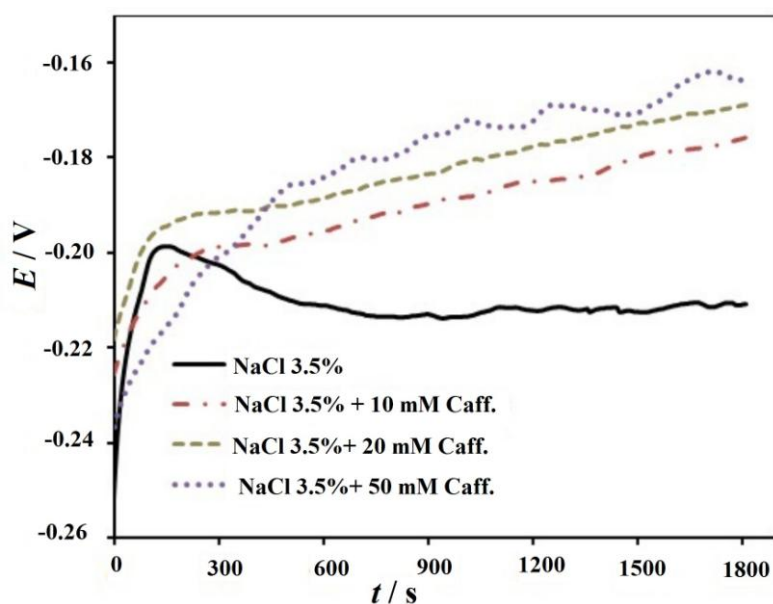


**Figure 1.** Potential vs. time response for Ni surface in 3.5% NaCl solution in the presence and absence of different concentration of the caffeine inhibitor.

Figure 1 shows that the OCP shift to more noble potentials with time and with the increase of the caffeine concentration. The increase of the OCP towards noble potentials is due to the adsorption of the inhibitor onto the nickel surface.

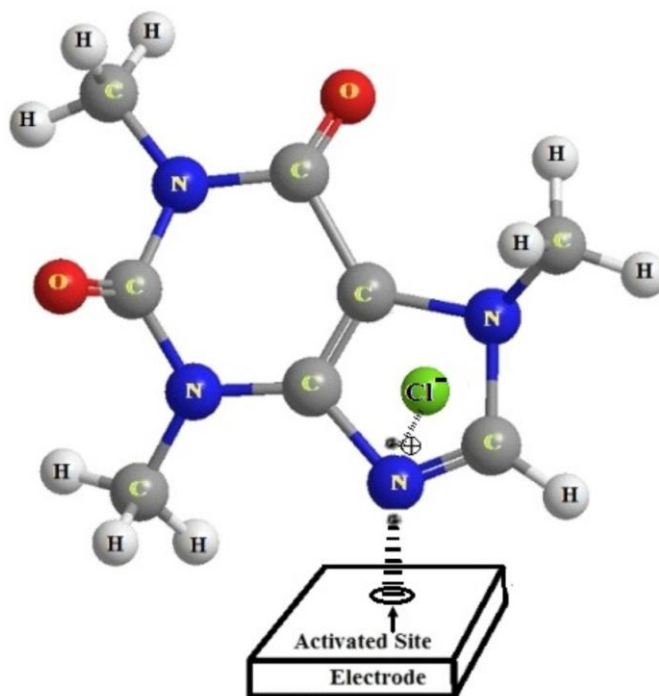


**Figure 2.** A schematic model for the adsorption of caffeine on nickel surface with the presence of  $\text{Cl}^-$ .

It can be proposed that the caffeine adsorption onto the nickel surface occurs with the release of electron cloud density from the lone pair of the nitrogen atom (particularly the electron rich  $\text{N}=\text{C}$  in the caffeine molecule) to the nickel surface (Fig. 2). The caffeine molecules prefer to adsorb on the activated sites ( $\text{Ni}^+_{\text{ad}}$ ) as soon as Step 1 (Eq. 3) occurs. This is because the caffeine adsorption will be stronger if the electron cloud density on the nitrogen atom pairs up with the  $\text{Ni}^+_{\text{ad}}$  active sites, resulting in an electrostatic interaction. Initially, Step 1 occurs before the adsorption of the caffeine molecule and this is shown in Fig. 1 where the OCP has negative values at the beginning. As soon as the adsorption of the caffeine molecule on the activated site ( $\text{Ni}^+_{\text{ad}}$ ) takes place, the OCP becomes more positive due to the electron charge density transfer from the nitrogen atom of the adsorbed caffeine molecule to the activated site ( $\text{Ni}^+_{\text{ad}}$ ) on the Ni surface. The positive charge density on the caffeine nitrogen atom on the opposite side of the nickel surface can prevent the  $\text{Cl}^-$  from approaching the nickel surface through binding with an electrostatic interaction with the  $\text{Cl}^-$  and also by the stereochemical hindrance of the caffeine molecule as shown in Fig. 2.

The nickel activated site ( $\text{Ni}^+_{\text{ad}}$ ) with the presence of caffeine adsorption behaves like a battery cathode during discharge. During the battery discharge, the cathode is positively charged and receives electrons. Quite similar to a battery cathode during discharge, the OCP of the nickel surface moves

towards positive potentials for longer times due to the transfer of the negative charges from the caffeine adsorption (Fig. 1).

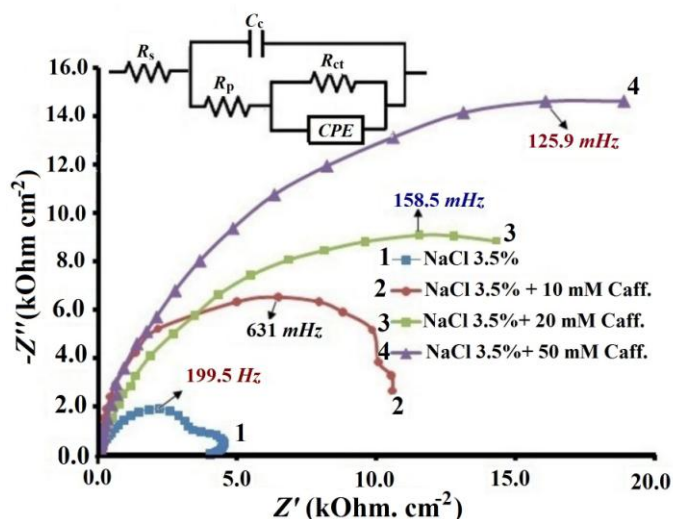


**Figure 3.** Nyquist plots for Nickel plates in 3.5% NaCl solution in the absence and presence of different concentration of caffeine. The straight line represents the simulation while the symbols represent the experimental data.

Electrochemical impedance spectroscopy (EIS) measurement was done immediately after the OCP measurement for each sample. The same solution was used to investigate the corrosion behaviour of Ni in the presence of various amounts of caffeine. Figure 3 shows that the diameter of the semi-circle in the Nyquist plots increase with the increase of the caffeine inhibitor concentration. As shown in Fig. 3, the caffeine inhibitor does not affect the solution resistance ( $R_s$ ). From the comparison of the simulation and experimental data of the nickel corrosion with the presence of caffeine, the most accurate equivalent circuit model for all the semicircles in the Nyquist plots is  $R_s(C[R_p(R_{ct}Q)])$ . Instead of the pure capacitance ( $C$ ), a constant phase element ( $CPE$ , denoted as  $Q$  in the circuit) is introduced in the simulation process to obtained good agreement between simulated and experimental data. The impedance ( $Z$ ) of the  $CPE$  is defined as  $Z_{CPE} = [Q(i\omega)^n]^{-1}$ , where  $Q$  ( $\Omega^{-1} s^n cm^{-2}$ ) is the combination of properties related to both the surface and the electroactive species independent of frequency [25, 26]. Thus  $Q$  will be closer to capacitance if “ $n$ ” becomes closer to 1. The “ $n$ ” value also depends on the surface roughness. The Nyquist plot for nickel corrosion in the presence of  $Cl^-$  without the inhibitor is similar to the results obtained by Keddad for nickel corrosion in sulphate media [32]. The presence of an inductive semi-circle at lower frequencies is due to the relaxation process from the adsorption of a chemical species [33-35]. In this work, the inductive semi-circle is due to the adsorption of the  $Ni^{2+}$  ions onto the Ni surface and is shown in the reverse of Step 2 in Eq. 4.

The equivalent circuit model can be explained as follows.  $R_s$  is the solution resistance between the WE and the RE.  $R_p$  is the pore resistance which is due to the corrosion of the nickel surface resulting in pore formation through the bulk metal.  $C$  is the surface capacitance of the pores from the intake of water and ions into the pores and  $R_p$  and  $C$  forms the first parallel combination. The second

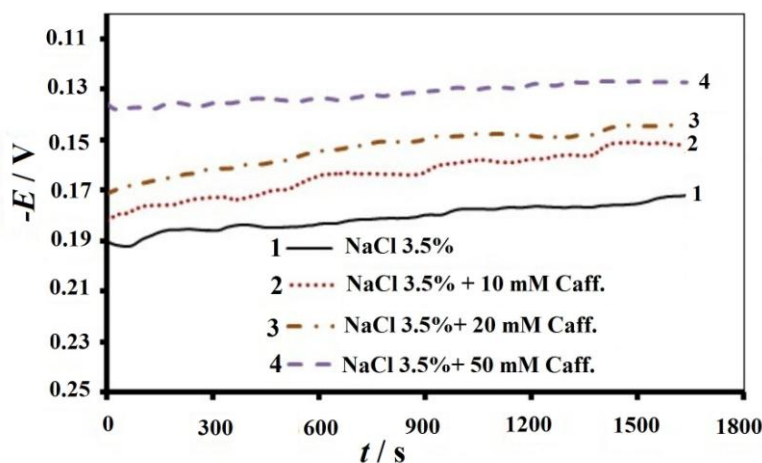
parallel combination is for the charge transfer resistance ( $R_{ct}$ ) and  $CPE$ , which is in series with the  $R_p$ . The  $CPE$  is often approximated to the double layer capacitance which occurs with the charge transfer process.  $R_{ct}$  is the charge transfer resistance which occurs across the Ni electrode/electrolyte interface and thus the  $R_{ct}$  value is the measure of the corrosion reaction which occurs across the electrode/electrolyte interface [25, 26].

Table 1 gives the parameters such as  $C$ ,  $R_{ct}$ ,  $n$ , and  $CPE$  values obtained from the simulation procedure, which shows that  $R_{ct}$  values increase with the presence of higher concentration of inhibitor and is consistent with the OCP results. Table 1 also shows that the capacitance increase with the increase of the additive concentration. As explained in the beginning of this section, the lone pair electrons of the nitrogen atom is donated to the nickel surface as soon as Step 1 occurs and thus providing a strong bonding through the electrostatic interaction between the charged nickel surface (activated site  $Ni^{+}_{ad}$ ) and the charged inhibitor. The increase of the inhibitor concentration will result in more charged inhibitor adsorption on the activated site on the nickel surface and increase the capacitance value due to the electrostatic interaction between the  $Ni^{+}_{ad}$  activated site and the caffeine molecules, as given in Table 1.

**Table 1.** Electrochemical impedance parameters for Ni plates in chloride bath in the presence and absence of caffeine.

[Caffeine]	$R_{ct}$ (k $\Omega$ cm <sup>2</sup> )	$C$ ( $\mu$ F cm <sup>-2</sup> )	$CPE$ Q ( $\mu$ F cm <sup>-2</sup> )	$n$
0 mM	4.26	20.2	420	0.899
10 mM	12.3	12.04	54.4	0.718
20 mM	25.2	6.85	37.1	0.763
50 mM	37.8	4.13	26.8	0.790

### 3.2. Electrochemical noise analysis (ENA)



**Figure 4.** Typical potential noise-time response on the nickel surface in 3.5% NaCl solution in the presence and absence of the caffeine inhibitor.

Electrochemical noise analysis is done on the nickel surface immediately after EIS analysis as a non-destructive technique. This technique is based in both the frequency and time domain. A typical signal pattern of the potential fluctuation in the time domain for 1675 s is given in Fig. 4. Figure 4 shows that the potential moves to positive regions with the increase of inhibitor concentration and this is consistent with the OCP results.

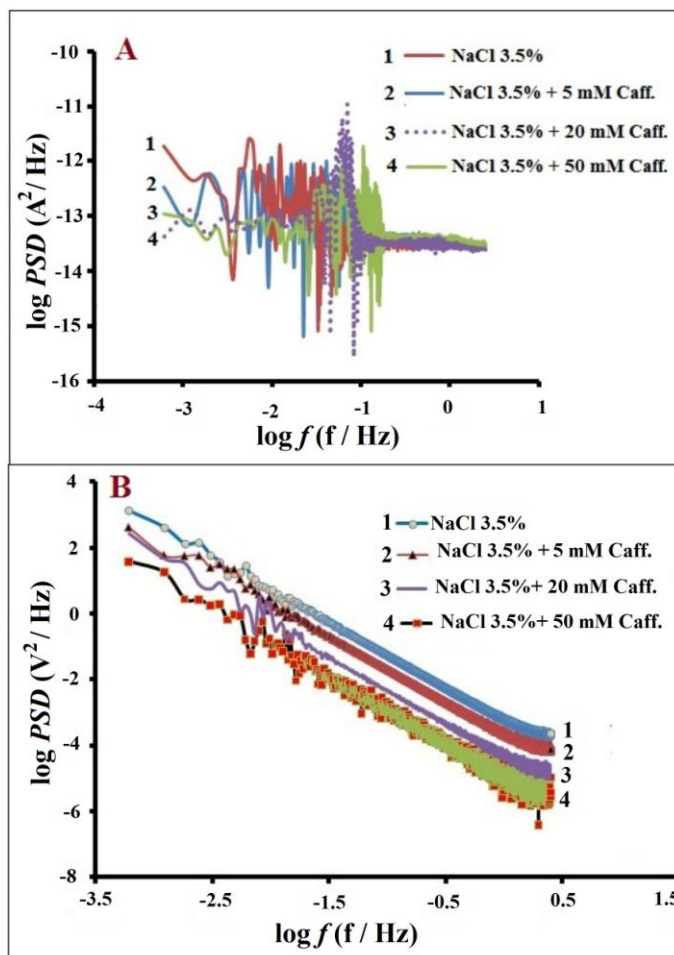


**Figure 5.** Power spectral density plots for A) Current, and B) Potential; for Ni plate in chloride solution in the absence and presence of caffeine.

Figure 5 shows the fluctuation of current and potential with time for nickel surface in various corrosive solutions. Transformation of electrochemical data ( $E$  and  $I$ ) using the Fourier frequency transformation ( $FFT$ ) method gives the plot of power spectra densities ( $PSDs$ ) vs ( $\log f$ ). Figure 5 (A, B) shows the simulated results for both potential and current in the frequency domain.

Figure 5 shows that the  $PSD$  plots are similar for all analysed surfaces. However, the values are different in the low frequency region (2 mHz). The corrosion rate is proportional to the value of spectral noise resistance ( $R_{sn}$ ) at low frequency (2 mHz). This factor ( $R_{sn}$ ) can be calculated from  $PSDs$  of potential and current and is defined as [23]:

$$R_{sn} = \frac{|V_{FFT(f)}|}{|I_{FFT(f)}|} = \left( \frac{V_{PSD(f)}}{I_{PSD(f)}} \right)^{1/2} \quad (5)$$

where the fluctuation of the potential and current noise are given by  $V_{FFT(f)}$  and  $I_{FFT(f)}$  respectively.  $V_{PSD}$  and  $I_{PSD}$  are the corresponding  $PSD$  plots for the  $V_{FFT(f)}$  and  $I_{FFT(f)}$  respectively. The estimation of corrosion rate from the electrochemical noise data Eq (5) can be given as [23]:

$$I_{corr.} = - (2.67 \times 10^{-8}) (PSD_{(I)}^{0.5})^{-0.29} \quad (6)$$

where  $I_{corr.}$  and  $PSD_{(I)}$  are the corrosion current ( $\text{Am}^{-2}$ ) and  $PSD$  value of the current at 2 mHz. The calculated corrosion rate (Table 2) shows that the corrosion rate diminishes with the increase of caffeine in the corrosive solution. The mechanism of corrosion can be investigated from the localized index ( $LI$ ) which it is defined as the ratio of the standard deviation of the current ( $\delta_I$ ) to the root mean square of the current ( $I_{rms}$ ) [23]:

$$LI = \frac{\delta_I}{I_{rms}} \quad (7)$$

$$\delta_I = \sqrt{\frac{\sum_n^N (I_n - \bar{I})^2}{N-1}} \quad (8)$$

where  $I_n$  is the current data pairs,  $\bar{I}$  is the mean value of the recorded current noise, and  $N$  is the total number of data points. Rothwell and Eden [27, 28] have suggested that the value of  $LI$  is related the corrosion mechanism i.e. the  $LI$  values between 0.001 and 0.01 are for uniform corrosion. The  $LI$  values between 0.1 and 1.0 are for localized corrosion, while  $LI$  values between 0.01 and 0.1 are for mixed corrosion. From Table 2, the  $LI$  values suggest that a uniform corrosion mechanism occurs with the presence of caffeine in the corrosive solution. The noise resistance ( $R_n$ ) is another useful parameter which can be derived from the standard deviation of both current ( $\delta_I$ ) and potential ( $\delta_V$ ) [23]:

$$\delta_V = \sqrt{\frac{\sum_n^N (V_n - \bar{V})^2}{N-1}} \quad (9)$$

$$R_n = \frac{\delta_V}{\delta_I} \quad (10)$$

where  $V_n$  is the potential data pairs,  $\bar{V}$  is the mean value of the recorded current noise. Mahjani et al. [24] have reported that  $R_n$  values from ENA are equivalent to charge transfer resistance ( $R_{ct}$ ) from the EIS. Significantly, from Tables 1 and 2, it can be shown that the changes of the  $R_n$  (EN) and  $R_{ct}$  (EIS) with the caffeine concentration are consistent with each other.

**Table 2.** The electrochemical noise data in the presence and absence of caffeine in 3.5% NaCl corrosive solution.

ECN	0 mM	5 mM	10 mM	20 mM	40 mM	50 mM
STDV $\times 10^{-9}(I)$	0.01	2.09	1.57	2.15	2.02	1.55
STDV $\times 10^{-3}(V)$	4.83	4.84	4.90	6.95	7.4	6.65
$I_{av.} \times 10^{-10}$	0.041	1.88	2.38	1.12	1.05	1.78
$V_{av.} \times 10^{-2}$	16.37	18.09	15.56	16.46	15.36	2.30
Rn ( $k\Omega\text{ cm}^{-2}$ )	10.11	23.12	31.26	32.35	36.71	42.80
LI	0.91	0.099	0.0998	0.0999	0.0100	0.0996
CR $\times 10^{-3}$ (mpy)	53.8	5.23	4.82	3.66	2.51	1.61

### 3.3. Potentiodynamic polarization

Potentiodynamic polarization was done on nickel surface in 3.5% NaCl containing different amounts of caffeine (0-50 mM) and is shown in Fig. 6. The electrochemical parameters such as the corrosion rate ( $CR$ ), corrosion potential ( $E_{corr}$ ), corrosion current ( $I_{corr}$ ) and Tafel slope constants from the potentiodynamic measurements are given in Table 3.

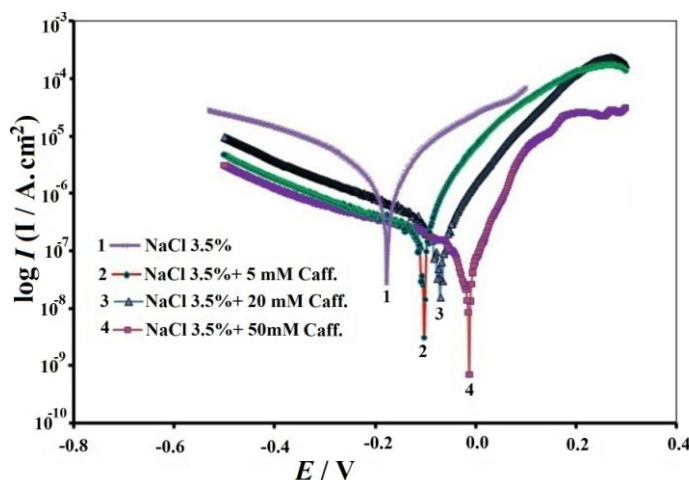


**Figure 6.** Polarization curves for the corrosion of Ni surface in 3.5% NaCl in the absence and presence of various amount of caffeine.

The Tafel slopes  $\beta_a$  and  $\beta_c$  can be determined from the anodic and cathodic curves respectively. The corrosion current and corrosion potential are obtained from the intersection of the Tafel slope lines, and the corrosion rate can be calculated from the Stern-Geary equation. Fig. 6 shows that the  $E_{corr}$  shifts to positive regions with the increase of caffeine in the corrosive solution. This result is also consistent with the OCP and ENA results. Table 3 also shows that the corrosion rate decrease with the increase of caffeine concentration which also consistent with the OCP, EIS and ENA measurements.

**Table 3.** Electrochemical polarization parameters and the inhibition efficiencies of Ni in 3.5% NaCl solution in the presence and absence of different concentrations of caffeine.

NaCl 3.5% contained:→	0 mM Caff.	5 mM Caff.	20 mM Caff.	50mM Caff.
$\beta_a$ (V/dec)	0.348	0.305	0.047	0.344
$\beta_c$ (V/dec)	0.207	0.055	0.203	0.06
$I_{corr.}$ (A/cm <sup>2</sup> )	$3.20 \times 10^{-6}$	$2.03 \times 10^{-7}$	$1.84 \times 10^{-7}$	$1.03 \times 10^{-7}$
$E_{corr.}$ (V)	-0.177	-0.099	-0.014	-0.011
$R_p$ (Ohm)	$9.74 \times 10^3$	$3.60 \times 10^4$	$2.27 \times 10^4$	$8.69 \times 10^4$
CR (mm/year)	$3.43 \times 10^{-2}$	$2.17 \times 10^{-3}$	$1.97 \times 10^{-3}$	$1.10 \times 10^{-3}$
IE%	0	93.68	94.26	96.80

Surface coverage ( $\theta$ ) and inhibition efficiency ( $IE$ ) are directly proportional to the corrosion behavior of surfaces which can be defined by the following equation [22]:

$$IE\% = [1 - W_2 / W_1] \times 100 \quad (11)$$

Where  $W_1$  and  $W_2$  are the corrosion rates in the absence and presence of the inhibitor respectively. The corrosion parameters determined from the Tafel plots are listed in Table 3. Table 3 shows that the inhibition efficiency increases from 93.68 to 96.80 with the increase of caffeine concentration.

### 3.4. Field Emission Scanning Electron Microscopy (FESEM) analysis

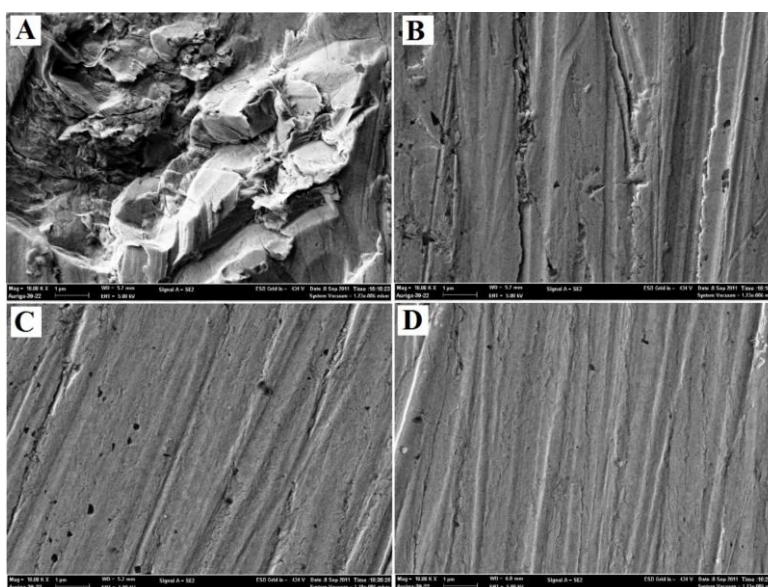


**Figure 7.** FESEM images (10000X) of the nickel surface after immersion in 3.5% NaCl solution for 2 weeks with: (A) the absence of caffeine, B) 5 mM caffeine, C) 20 mM caffeine, and D) 50 mM caffeine.

Figure 7A-7D show the FESEM images of the nickel surface exposed in the corrosive solutions in the absence and the presence of different concentrations (5-50 mM) of caffeine for 2 weeks. Figure 7A shows pits and cavities on the nickel surface in the absence of caffeine due to the attack of the aggressive ions ( $\text{Cl}^-$ ). Figure 7B-7D show that the cavity and pit formation decrease with presence of caffeine in the corrosive solution. These images are consistent with the electrochemical results of OCP, EIS, ENA and Tafel plots in the previous sections.

#### 4. CONCLUSION

The influence of caffeine on the corrosion inhibition of nickel surface is investigated by AC and DC techniques such as EIS, Tafel, OCP and ENA. Experimental data from the OCP and the EIS results suggest that the adsorption of the caffeine molecules occurs after the formation of the activated sites ( $\text{Ni}^+_{\text{ad}}$ ) on the Ni surface. From the EIS results, it was found that the caffeine does not only adsorb on the nickel surface but also participates in a negative charge density transfer to the activated sites ( $\text{Ni}^+_{\text{ad}}$ ) on the Ni surface which results in an electrostatic interaction between the surface and the adsorbed caffeine molecules. This can be seen from the EIS results where the capacitance increases with the concentration of the inhibitor. The adsorption of the caffeine also provides a stereo-chemical hindrance against the  $\text{Cl}^-$  ions from attacking the Ni surface. The inhibition efficiency ( $IE\%$ ) calculated from the polarization curves gives an efficiency of more than 90%. The FESEM images of the nickel surface shows an improved surface morphology free from cavity and pit formation with the addition of caffeine in the corrosive solution.

#### ACKNOWLEDGEMENTS

The authors would like to thank University of Malaya and Ministry of Higher Education for financial support through research grants UMRG091/10AFR, FRGS FP039 2010B and HIR F000004-21001.

#### References

1. M. Ebadi, W. J. Basirun, Y. Alias, M. R. Mahmoudian and S. Y. Leng, *Mater. Charact.*, 66 (2010) 46.
2. M. Ebadi, W. J. Basirun and Y. Alias, *J. Chem. Sci.* 2010, 122 (2) (2010) 279.
3. M. Ebadi, W. J. Basirun, Y. Alias and M. R. Mahmoudian, *Chem. Cent. J.* 4 (1) (2010) 14.
4. M. Ebadi, W. J. Basirun, Y. Alias and M. R. Mahmoudian, *Metall. Mater. Trans A*, 42A (2011) 2402.
5. I. Ahmad, R. Prasad and M. A. Quraishi, *Corros. Sci.*, 52 (2010)1472.
6. D. K. Yadav, B. Maiti and M. A. Quraishi MA, *Corros. Sci.*, 52 (2010) 3586.
7. S. Edrah and S. K. Hasan, *J. Appl. Sci. Res.*, 6(8) (2010) 1045.
8. Y. J. Tan, S. Bailey and B. Kinsella, *Corros. Sci.*, 38 (1996) 1681.
9. M. Z. A. Rafiquee, S. Nidhi, K. Sadaf and M. A. Quraishi, *Mater. Chem. Phys.*, 107 (2008) 528.
10. E-S. M. Sherif, R. M. Erasmus and J. D. Comins, *J. Coll. Inter. Sci.*, 306 (1) (2007) 96.
11. R. F. V. Villamil, G. G. O. Cordeiro, J. Matos, ED'Elia and S. M. L. Agodtinho, *Mater. Chem. Phys.*, 78 (2) (2003) 448.

12. E. S. Lisac, A. Gazivoda and M. Madzarac, *Electrochim. Acta*, 47 (26) (2002)4189.
13. J. M. Bastidas, P. Pinilla, E. Cano, J. L. Polo and S. Miguel, *Corros. Sci*, 45 (2) (2003) 427.
14. Y-C. Wu, P. Zhang, H. W. Pickering and D. L. Allara, *J. Electrochem. Soc.*, 140 (10) (1993) 2791.
15. E. M. Sherif and Su-M. Park, *Electrochim. Acta*, 51 (7) (2006)1313.
16. E. M. Sherif and S-M. Park. *J. Electrochem. Soc.*, 152 (10)(2005) B428.
17. M. Ehteshamzadeh, T. Shahrabi and M. Hosseini. *Anti-Corros. Meth. Mater*, 53 (5) (2006) 296.
18. A. A. Nazeer, A. S. Fouda and E. A. Ashour, *J. Mater. Environ. Sci*, 2 (1) (2011) 24.
19. J. B. Matos, L. P. Pereira, S. M. L. Agostinho, O. E. Barcia, G. G. O. Cordeiro and E. D'. Elia, *J. Electroanal. Chem*, 570 (1) (2004) 91.
20. M. M. Antonijevic and M. B. Petrovic, *Int. J. Electrochem. Sci*, 3 (2008) 1.
21. T. Fallavena, M. Antonow and R. S. Goncalves, *Appl. Surf. Sci*, 253(2) (2006) 566.
22. S. Rajendran, S. Vaibhavi, N. Anthony and D. C. Trivedi, *Corros. Sci*, 59 (6) (2003) 529.
23. M. G. Mahjani, M. Sabzali, M. Jafarian and J. Neshati, *Anti-Corros. Meth. Mater*, 55 (4) (2008) 208.
24. J. R. Kearns, J. R. Scully, P. R. Roberge, D. L. Reichert and J. L. Dawson, *Electrochemical noise measurement for corrosion applications*. ASTM, ISBN 1-8031-2032-X, (1996).
25. M. R. Mahmoudian, W. J. Basirun, Y. Alias and M. Ebadi, *Appl. Surf. Sci*, 257, 20(1) (2011) 8317.
26. M. R. Mahmoudian, W. J. Basirun and Y. Alias, *Prog. Org. Coat*,71 (1) (2011) 56.
27. M. G. Mahjani , M. Sabzali , M. Jafarian , J. Neshati, *Anti-Corros. Meth. Mater*, 55 (4) (2008) 208.
28. A. N. Rothwell and D. A. Eden. *Electrochemical noise techniques for determining corrosion rates and mechanisms*, Houston, TX: NACE (1992).
29. Z. Shahnavaaz, W. J. Basirun and S. M. Zain, *Anti-Corros. Meth. Mater*, 57 (1) (2010) 21.
30. N. Sato and G. Okamoto, *J. Electrochem. Soc.*, 110 (1963) 605.
31. N. Sato and G. Okamoto, *J. Electrochem. Soc.*, 111 (1964) 897.
32. M. Keddad, H. Takenouti and N. Yu, *J. Electrochem. Soc.*, 132 (11) (1985) 2561.
33. M. Keddad, O. R. Mattos and H. Takenouti, *J. Electrochem. Soc.*, 128 (1981) 257.
34. H. H. Hassan, E. Abdelghani and M. A. Amin, *Electrochim. Acta*, 52 (2007) 6359.
35. M. A. Amin, S. S. Abd. El-Rehim, E. E. F. El-Sherbini and R. S. Bayyomi, *Electrochim. Acta*, 52 (2007) 3588.